

# Impact of MODIS atmospheric motion vectors on a global NWP system

J. Le Marshall<sup>1</sup>, J. Jung<sup>1,2</sup>, T. Zapotocny<sup>1,2</sup>, C. Redder<sup>1,3</sup>, M. Dunn<sup>1,4</sup>,  
J. Daniels<sup>1,5</sup> and Lars Peter Riishojgaard<sup>1,3</sup>

<sup>1</sup>Joint Center for Satellite Data Assimilation, Camp Springs, MD, USA

<sup>2</sup>Cooperative Institute for Meteorological Satellite Studies (CIMSS), Madison, WI, USA

<sup>3</sup>Global Modeling Assimilation Office, NASA/GSFC (GMAO), Greenbelt, MD, USA

<sup>4</sup>LaTrobe University, Victoria, Australia

<sup>5</sup>NOAA/NESDIS STAR, Camp Springs, MD, USA

(Manuscript received January 2007; revised January 2008)

## Introduction

Atmospheric motion vectors (AMVs) generated using observations in the infrared (11  $\mu\text{m}$ ) and the water vapour absorption band (6.7  $\mu\text{m}$ ) taken by the Moderate Resolution Imaging Spectrometer (MODIS) instrument on the National Aeronautics and Space Administration (NASA) Aqua and Terra satellites have been assimilated into the National Centers for Environmental Prediction (NCEP) Global Forecast System (GFS) and have been shown to improve global forecasts. These AMVs provide vital wind information in the data-sparse polar regions of the globe, where the use of remote sensing data is often difficult. Several periods have been examined including August and September 2004 and the International MOWSAP (MODIS Winds Special Acquisition Period), January and February 2004. This assimilation study was part of the initial testing for the operational National Oceanic and Atmospheric Administration/National Environmental Satellite Data Information Service (NOAA/NESDIS) MODIS AMV system, which is now used to generate these winds operationally. The MODIS AMVs are distributed via the Global Telecommunication System (GTS) for the international community. The MODIS-based AMVs have been characterised in terms of error and correlated error and data impact tests have also been undertaken using MODIS wind data in analyses up to the second-last analysis in the assimilation cycle, as this represents the current operational

availability of the wind data at NCEP. The tests summarised here show positive forecast impact on the GFS at middle and high latitudes in both hemispheres. It was also noted use of the AMVs provided an impact in tropical latitudes and in the Atlantic basin which resulted in improved tropical cyclone track forecasts during the 2004 hurricane season.

The impact of these winds, used up to the second-last analysis in the GFS forecast cycle, has resulted in their introduction into the Operational Global Forecast Suite at NCEP. In effect this study has not only demonstrated the utility of the winds for operational numerical weather prediction (NWP), but also the considerable transfer of information through the operational analysis background fields.

## The polar winds

Early methods for generating AMVs at high latitudes from polar-orbiting Operational Environmental Satellites (POES) are discussed in Turner and Warren (1989), Herman (1993) and Herman and Nagle (1994). The methods used for generating cloud and water vapour based polar AMVs using MODIS observations from the NASA Aqua and Terra satellites (Key et al. 2003, 2004; Daniels et al. 2004) are similar to those used with sequential infrared and water vapour band observations from the Geostationary Operational Environmental Satellites (GOES) (Nieman et al. 1997; Velden et al. 1997; Le Marshall et al. 2003). To generate the winds used here, infrared (11  $\mu\text{m}$ ) and water vapour (6.7  $\mu\text{m}$ ) band imagery from three sequential polar

---

Corresponding author address: J. Le Marshall, Centre for Australian Weather and Climate Research, Bureau of Meteorology, GPO Box 1289, Melbourne, Vic. 3001, Australia.  
Email: j.lemarshall@bom.gov.au

overpasses by the Terra and Aqua satellites were first remapped to polar stereographic projection. Strong gradient features in the sequential infrared and water vapour imagery were then used as potential targets for tracking. Targets were selected from the central image. The method for estimating velocity relied on measuring the target displacement which minimises brightness temperature differences between the initial and final target in subsequent images. The search for the targets was aided by use of the forecast wind fields to determine the search areas for target location. The estimation of these winds presents some additional problems not faced with geostationary image-based winds, including dealing with loss of vector numbers because of the larger time intervals between images. Height assignment of the vectors involved using the Infrared (IR) Window Method, the Water Vapour (WV) Intercept Method, and for clear water vapour imagery the coldest pixels were used to define the observation level. In all cases the temperature profile from the NCEP Global Forecast System was used to estimate the AMV altitude from the cloud or clear air tracer temperature. The near-isothermal nature of parts of the polar troposphere, surface inversions and the difficulty in using remotely sensed data over polar regions can sometimes make this process difficult.

The error characteristics of the MODIS polar AMVs have been determined. Typical accuracy of the vectors available for data assimilation is shown in Table 1. The values recorded are the number of obser-

vations collocated with radiosondes, the mean magnitude of vector difference (MMVD), the RMS vector difference (RMSVD) and speed bias between the MODIS AMVs and radiosondes within 150 km, where the Quality Indicator (QI) associated with the AMVs is greater than 0.85. The accuracy of the vectors has been found to make them useful for NWP, although room for some improvement (e.g. in middle-level bias) still remains.

An indication of the accuracy of the MODIS AMV height assignment methodology is seen in Fig. 1, which shows the distribution of the pressure level of best fit compared to collocated radiosonde profiles, for AMVs determined to be at middle, low and high levels by the AMV generation system.

Figure 1(a) shows the distribution of the level of best fit, compared to collocated contemporaneous radiosonde profiles, for vectors with a Quality Indicator (QI - Holmlund 1998; Holmlund et al. 2001) in the range of 0.85 to 1. Figure 1(b) shows the distribution of the level of best fit, compared to collocated contemporaneous radiosonde profiles, for vectors with Expected Errors (EE - Le Marshall et al. 2004) less than 5 m/s.

In relation to Fig. 1(a), northern hemisphere AMVs for the period May 2005 to June 2006, originally height assigned to the 500 ± 50 hPa range, with QI in the range 0.85 – 1.0, have been used to produce a distribution of the level of best fit compared to collocated contemporaneous radiosondes. Similar plots have been made for vectors in the ranges 300 ± 50

**Table 1. Comparison of radiosonde wind estimates with Terra and Aqua based MODIS AMVs, collocated within 150 km over high latitudes for the period 5 May 2005 to 10 January 2006 inclusive, where the AMV QI > 0.85. (IR = 11 µm based winds, WV = 6.7 µm based winds and MMVD = mean magnitude of vector difference (m s<sup>-1</sup>).**

Type		AQUA IR	AQUA WV	TERRA IR	TERRA WV
Low 999-700 hPa	No. of obs.	142	N/A	80	N/A
	MMVD (m s <sup>-1</sup> )	3.92	N/A	3.58	N/A
	rms vec. diff. (m s <sup>-1</sup> )	4.57	N/A	4.02	N/A
	Speed bias (m s <sup>-1</sup> )	-0.30	N/A	-0.03	N/A
Middle 699-400 hPa	No. of obs.	342	558	287	485
	MMVD (m s <sup>-1</sup> )	4.38	4.34	4.20	4.30
	rms vec. diff. (m s <sup>-1</sup> )	4.93	4.90	4.79	4.85
	Speed bias (m s <sup>-1</sup> )	-1.01	-0.72	-0.35	-0.24
High 399-150 hPa	No. of obs.	106	358	76	345
	MMVD (m s <sup>-1</sup> )	4.71	4.96	4.81	4.28
	rms vec. diff. (m s <sup>-1</sup> )	5.22	5.55	5.26	4.83
	Speed bias (m s <sup>-1</sup> )	-0.80	-0.65	-0.50	-0.34

**Fig. 1(a)** Distribution of levels of best fit compared to a collocated radiosonde profile for AMVs with pressure altitudes in the ranges  $500 \pm 50$  hPa (mid level),  $300 \pm 50$  hPa (high level) and  $850 \pm 50$  hPa (low level). In all cases, the AMV QI is in the range 0.85 to 1.0.

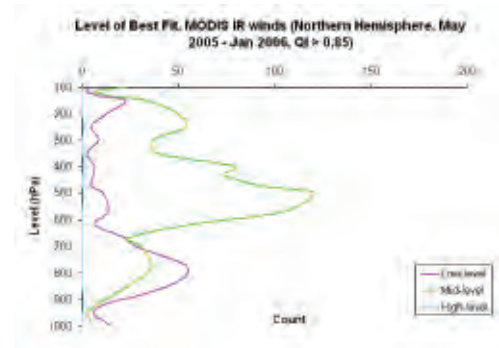
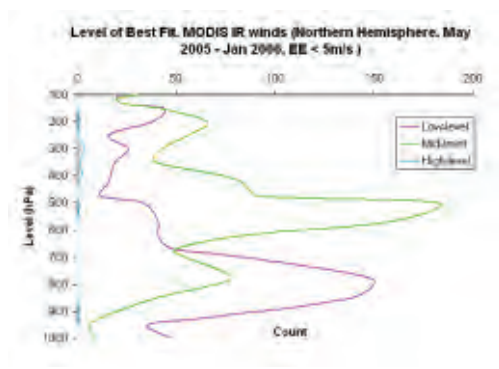


**Fig. 1(b)** Distribution of levels of best fit compared to a collocated radiosonde profile for AMVs with pressure altitudes in the ranges  $500 \pm 50$  hPa (mid level),  $300 \pm 50$  hPa (high level) and  $850 \pm 50$  hPa (low level). In all cases, the AMV EE is less than 5 m/s.



hPa and  $800 \pm 50$  hPa. It is clear that, although the majority of vectors are around the correct height, significant improvement can still be made in height assignment accuracy. Figure 1(b) is the corresponding plot for the northern hemisphere but with vectors selected using EEs in the range 0 – 5 m/s and, again, although the majority of height assignments and levels of best fit are consistent, there still exists a significant area for improvement. The figures also indicate that use of the EE has resulted in selection of more

vectors compared to use of the QI, for similar average MMVD (for example, in the mid-levels, the average MMVD for AMVs with QI > 0.85 is 4.3 m/s and for AMVs with EE > 5 m/s is 4.1 m/s). It also appears that use of the EE has resulted in a sharper and more appropriate vertical distribution of the AMVs.

In terms of estimating the correlated error (CE) of the AMVs, the separation of the vectors versus CE is plotted in Fig. 2 for IR and WV image based AMVs. A length scale (L) and CE, estimated using collocated contemporaneous radiosonde observations from a match file, have been associated with these vectors. The distribution of polar radiosonde stations used is shown in Key et al. (2003). The method used is documented in Le Marshall et al. (2004). The observed data (see, for example, Fig. 2) has been analysed, using an isotropic error correlation versus distance function, which is satisfactory for an initial application to data assimilation. The correlation function used to extrapolate to zero separation is the Second Order Auto Regressive (SOAR) function of Daley (1991).

$$R(r) = R_{00} + R_0(1 + r/L)e^{-r/L} \quad \dots 1$$

where  $R(r)$  is the error correlation, with fitting parameters  $R_{00}$  and  $R_0$  (greater than 0), length scale  $L$  and separation distance of the correlates  $r$ . Figures 2(a) and 2(b) show error correlation versus distance for IR and WV mid-level vectors using 10 km bins. The parameters  $R_{00}$  and  $R_0$ , the length scale ( $L$ ) and the CE of the SOAR functions fitted to the distance correlation functions are presented in Table 2.

The length scale for the MODIS polar high-level WV image based AMVs (107.6 km) is generally a little larger than for the GMS-5 (84.8 km) and southern hemisphere GOES (89.2 km) WV AMVs (Le Marshall et al. 2004). The analysis for MODIS IR image based AMVs indicates a larger length scale at lower compared to upper levels, as with GMS-5 and southern hemisphere GOES.

## Data assimilation

Wind observations from polar-orbiting satellites in polar latitudes have been used in a number of data assimilation studies, e.g., Bormann and Thépaut (2004), Riishojgaard and Zhu (2004), Kazumori and Nakamura (2004) and Sarrazin and Zaitseva (2004). In these studies, after careful quality control, thinning and error assignment, positive impact was demonstrated in both hemispheres, using winds available from the Cooperative Institute for Meteorological Satellite Studies (CIMSS) or NOAA/NESDIS.

**Fig. 2(a)** Error correlation versus distance (using 10 km bins), determined by comparison with radiosonde winds, for MODIS WV mid-level vectors (northern hemisphere, May 2005 to January 2006).

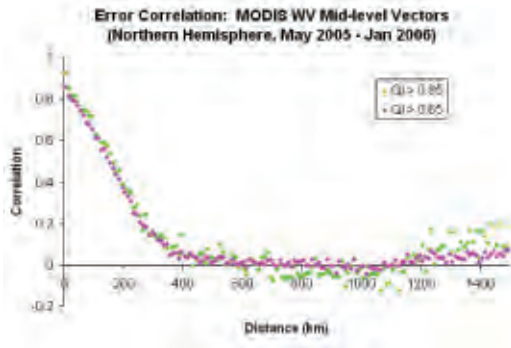


**Fig. 2(b)** Error correlation versus distance (using 10 km bins), determined by comparison with radiosonde winds, for MODIS IR mid-level vectors (northern hemisphere, May 2005 to January 2006).

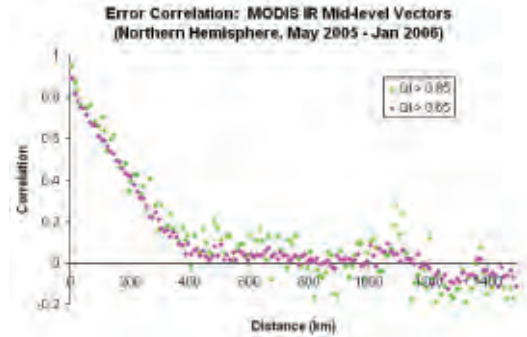


**Table 2(a).** Parameters of the SOAR function (Eqn 1) which best model the measured error correlations for the MODIS AMV types listed in the left column of the table. (QI = 0.65 to 1.)

Type	$R_{00}$	$R_0$	$L$ (km)	$CE$ ( $m s^{-1}$ )	$RMSD$ ( $m s^{-1}$ )
Low IR	-0.029	0.68	128.9	3.01	4.51
Mid IR	-0.010	0.82	113.1	4.16	5.07
High IR	0.029	0.78	117.7	4.28	5.49
Mid WV	0.010	0.85	95.3	4.29	5.05
High WV	-0.051	0.91	107.6	4.83	5.31

**Table 2(b).** Parameters of the SOAR function (Eqn 1) which best model the measured error correlations for the MODIS AMV types listed in the left column of the table.  $R_{00}$  is assumed to be 0. (QI = 0.65 to 1.)

Type	$R_{00}$	$R_0$	$L$ (km)	$CE$ ( $m s^{-1}$ )	$RMSD$ ( $m s^{-1}$ )
Low IR	0	0.77	123.6	3.47	4.51
Mid IR	0	0.84	120.3	4.26	5.07
High IR	0	0.83	98.6	4.56	5.49
Mid WV	0	0.89	100.4	4.49	5.05
High WV	0	0.95	100.8	5.04	5.31

Here, polar wind data generated by NOAA/NESDIS (Daniels et al. 2004) for the period 10 August – 23 September 2004 have been combined with the full NCEP operational database, including the satellite data listed in Table 3, and have been used with the NCEP Global Forecast System (Derber et al. 2003). The forecast model used was a T254, 64 level version of the operational GFS (November 2004 version). Forecasts from the system using MODIS AMV data

with the full operational database (MODIS) have been compared to forecasts using the full operational database only (Control). It is important to note that the MODIS wind data were used in all analyses in the assimilation cycling process except for the final analysis, where the MODIS data were not available operationally in time for that analysis (i.e. not available within the 2.5 hour operational cut-off). However, as the assimilation and forecast methodolo-

**Table 3. The satellite data used operationally within the NCEP Global Forecast System in 2004.**

HIRS sounder radiances	TRMM precipitation rates
AMSU-A sounder radiances	ERS-2 ocean surface wind vectors
AMSU-B sounder radiances	Quikscat ocean surface wind vectors
GOES sounder radiances	AVHRR SST
GOES, Meteosat	AVHRR vegetation fraction
atmospheric motion vectors	AVHRR surface type
GOES precipitation rate	Multi-satellite snow cover
SSM/I ocean surface wind speeds	Multi-satellite sea ice
SSM/I precipitation rates	SBUV/2 ozone profile and total ozone

gy used here was consistent with NCEP's operational methodology (Zapotocny et al. 2008), the information provided by MODIS still reached the final analysis through the operational analysis background field. The background field is a six-hour forecast from a late run of the last operational analysis, which is performed to pick up data which was not available at the operational cut off time of the GFS. This contains MODIS data which became available after the operational cut-off time for the GFS.

A similar experiment to the one cited above was run for the MOWSAP period, January and February 2004 and is also reported below.

## The forecasts

For the period 10 August to 23 September 2004, and also for the MOWSAP period, 1 January to 15 February 2004, a series of forecasts has been completed. Results for the August to September period are shown in Figs 3 and 4. Figure 3 shows the 500 hPa geopotential height Anomaly Correlation (AC) in the northern hemisphere high latitudes for the period 10 August to 23 September 2004. It shows an improvement in the AC for the period from the addition of MODIS data used over the polar latitudes. This is a similar result to that in the study by Riishojgaard and Zhu (2004), which used winds generated at the University of Wisconsin and employed the NASA Finite Volume Data Assimilation System. It is also consistent with the results of Bormann and Thépaut (2004), Kazumori and Nakamura (2004) and Sarrazin and Zaitseva (2004). Bormann and Thépaut reported positive impact from the use of University of Wisconsin generated winds for periods in 2001 and 2002, while Kazumori and Nakamura reported positive impact of Wisconsin AMVs in the northern hemisphere with summer and winter cases in 2003 and 2004, respectively. Sarrazin and Zaitseva also report positive impact from the MODIS AMVs for the MOWSAP period.

**Fig. 3** The 500 hPa geopotential height anomaly correlation for the northern hemisphere polar region (60°N – 90°N), for the GFS control and the GFS control including MODIS AMVs, for the period 10 August to 23 September 2004.

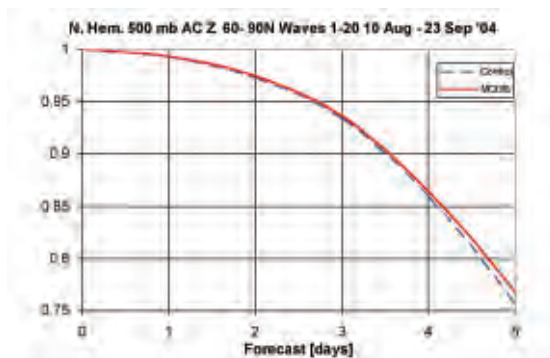
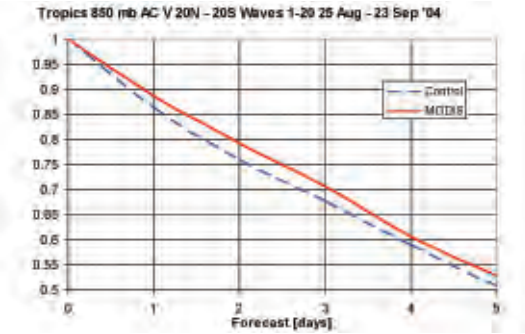


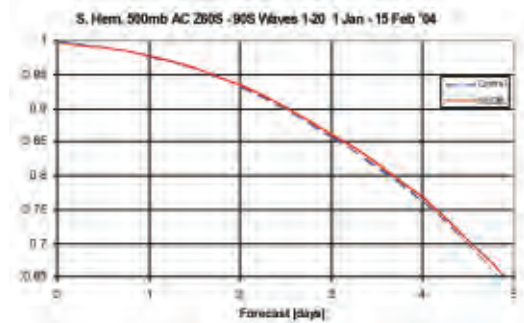
Figure 4 shows the 850 hPa tropical wind V-component AC values. In this study, it is clear that the MODIS winds, when cycled into the analysis system, have been able to reduce forecast errors even in the tropical belt, well away from the site of their estimation, at high latitudes. This is a notable result and indicates the utility of the MODIS AMVs in areas away from the polar regions, where the AMVs are generated and contribute to analysis.

In assessing the use of MODIS AMVs in the operational GFS at NCEP, northern hemisphere tropical cyclone track forecast accuracy for the MODIS assimilation runs was checked as part of the standard forecast verification process. The results in the Atlantic Basin for this study period are summarised in Table 4. It is clear, in this study, that an improvement in tropical cyclone track forecast accuracy has also accompanied the use of MODIS AMVs for the study period. The results, here, for the tropics are supported

**Fig. 4** The 850 hPa meridional wind component anomaly correlation for the tropical belt (20°N to 20°S), for the GFS control and the GFS control including MODIS AMVs, for the period 10 August to 23 September 2004.



**Fig. 5** The 500 hPa geopotential height anomaly correlation for the southern hemisphere polar region (60°S – 90°S), for the GFS control and the GFS control including MODIS AMVs, for the period 1 January to 15 February 2004.



by the study of Sarrazin and Zaitseva (2004), which showed the tropical influence of the MODIS AMVs in the Canadian data assimilation system (see their Fig. 6) and by the study of Kazumori and Nakamura (2004), which showed better predictions of typhoon tracks with the use of MODIS winds, although for a very limited sample.

In addition to the August and September 2004 study discussed above, the impact of MODIS AMVs was also examined for the MOWSAP period, 1 January to 15 February 2004, with similar results. Figure 5 shows the 500 hPa geopotential height AC for the southern hemisphere high latitudes for that period. Again, a gain in forecast skill with the use of MODIS winds was demonstrated.

## Summary and conclusions

NOAA/NESDIS are now routinely generating polar AMVs using overlapping IR and WV images from the MODIS instruments on the NASA EOS satellites Terra and Aqua. The techniques used are simi-

lar to those used at the University of Wisconsin (Key et. al. 2003) in most ways. One key difference at the time of this study was that the initial targets used for tracking were first identified in the middle image used in the production of these winds at NESDIS. Because of the time interval between images used in wind generation and the average cloud tracer lifetime, using tracers in the central image improves the wind yield and is now done by all polar wind processors.

The NOAA/NESDIS winds have been tested in NCEP's GFS during two periods. The late northern hemisphere summer of 2004 and the MOWSAP period. It was found that, on average, the MODIS AMVs improved forecasts in both the southern and northern hemispheres. It was found their influence also extended to tropical regions where it was noted they had a beneficial effect as shown in Fig. 4. It was also noted for this study that they had a beneficial effect on tropical cyclone track forecasts in the Atlantic Basin during the 2004 hurricane season. As a result of this study, these data are now used in the NCEP operational GFS.

**Table 4.** 2004 Atlantic basin average hurricane track errors (nm) from the NCEP GFS without MODIS AMVs (Cntrl) and with MODIS AMVs (Cntrl + MODIS).

Forecast period	00 h	12 h	24 h	36 h	48 h	72 h	96 h	120 h
Cntrl	13.2	43.6	66.5	94.9	102.8	157.1	227.9	301.1
Cntrl + MODIS	11.4	34.8	60.4	82.6	89.0	135.3	183.0	252.0
Cases (#)	74	68	64	61	52	46	39	34

In terms of future development, the real-time production of MODIS winds with improved error characterisation, including the Expected Error (EE) (Le Marshall et al. 2004) has been completed at NOAA/NESDIS and the AMVs are now part of the NESDIS test processing stream. The EE has recently been included in new MODIS AMV BUFR messages and the full system is being assessed in part using a real-time NWP impact trial.

In terms of the future availability of polar winds after the EOS Aqua and Terra satellite missions, there is currently no immediate operational polar-orbiting mission which will provide the 6.7  $\mu\text{m}$  imagery necessary to allow provision of real-time water vapour imagery based polar winds. Later versions of the Visible/Infrared Imager Radiometer Suite (VIIRS) on the National Polar-orbiting Environmental Satellite System (NPOESS) are expected to provide these data in the last half of the next decade. Infrared and visible imagery based winds from the Advanced Very High Resolution Radiometer (AVHRR) and line of sight winds from the Atmospheric Dynamics Mission – Aeolus Doppler wind lidar mission may lessen the consequences of losing observations in the water vapour absorption band before the VIIRS data become available.

In summary, it would appear that the MODIS AMVs provide analysis and forecast improvement from polar to tropical latitudes. The problem of timeliness is ameliorated by information transfer through the assimilation system background fields and, in this study, the impact in tropical regions was not only apparent in anomaly correlation fields but also manifest itself in an improvement in tropical cyclone track prediction. The MODIS winds are a significant contribution to the otherwise sparse polar wind database and are a valued part of a modern satellite database for operational data assimilation. The determination of the error characteristics of the winds, new data selection tools (e.g. EE) and current development work on height assignment, also indicate the quality of the winds available for operational assimilation systems is expected to improve.

## Acknowledgments

Many thanks are due to Ada Armstrong and Terry Adair for helping in the preparation of this manuscript.

## References

Bormann, N. and Thépaut, J.-N. 2004. Impact of MODIS polar winds in ECMWF's 4DVAR data assimilation system, European Centre for Medium-Range Weather Forecasts, Reading, United Kingdom. *Mon. Weath. Rev.*, 132, 929-40.

- Daley, R. 1991. *Atmospheric data analysis*. Cambridge University Press, Cambridge, UK. 460 pp.
- Daniels, J., Velden, C., Bresky, N. and Irving, A. 2004. Status of the NOAA/NESDIS Operations Satellite Wind Product System: Recent improvements, new products, product quality, and future plans. *Proc. Seventh Int. Winds Workshop* 1-17 June 2004, Helsinki. (EUMETSAT, ISBN 92-9110-067-6), 31-44.
- Derber, J.C., Van Delst, P., Su, X.J., Li, X., Okamoto, K. and Treadon, R. 2003. Enhanced use of radiance data in the NCEP data assimilation system. *Proc. 13th Int. TOVS Study Conference*. Ste. Adele, 29 October – 4 November, Canada 2003.
- Herman, L.D. 1993. High frequency satellite cloud motion at high latitudes, *Eighth Symposium on Meteorological Observations and Instrumentation*, Anaheim, CA, January 17-22, 1993, 465-8.
- Herman, L.D. and Nagle, F. W. 1994. A comparison of POES satellite derived winds techniques in the Arctic at CIMSS. *Proc. 7th Conference on Satellite Meteorology and Oceanography*, Monterey, CA, 6-10 June 1994, American Meteorological Society, Boston, MA, 1994, 444-7.
- Holmlund, K. 1998. The utilization of statistical properties of satellite-derived atmospheric motion vectors to derive quality indicators. *Weath. forecasting*, 13, 1093-104.
- Holmlund, K., Velden, C.S. and Rohn, M. 2001. Enhanced automated quality control applied to high-density satellite-derived winds. *Mon. Weath. Rev.*, 129, 517-29.
- Kazumori, M. and Nakamura, Y. 2004. MODIS polar winds assimilation experiments at JMA. *Proc. Seventh Int. Winds Workshop*, 1-17 June 2004, Helsinki (EUMETSAT, ISBN, 92-9110-067-6), 265-72.
- Key, J., Santek, D., Velden, C.S., Borman, N., Thépaut, J.N., Riishojgaard, L.P., Zhu, Y. and Menzel, W.P. 2003. Cloud-drift and water vapor winds in the polar regions from MODIS. *IEEE Trans. Geosci. Remote Sensing*, 41, 482-92.
- Key, J., Santek, D. and Velden, C. 2004. Atmospheric motion vector height assignment in the polar regions: issues and recommendations. *Proc. Seventh Int. Winds Workshop*, 1-17 June 2004, Helsinki (EUMETSAT, ISBN, 92-9110-067-6), 241-8.
- Le Marshall, J.F., Leslie, L.M., Seecamp, R. and Rea, A. 2003. High resolution space based wind observations. Estimation and application – a review. *Mausam*, 54, 1-12.
- Le Marshall, J.F., Rea, A., Leslie, L., Seecamp, R. and Dunn, M. 2004. Error characterization of atmospheric motion vectors. *Aust. Met. Mag.*, 53, 123-31.
- Nieman, S.J., Menzel, W.P., Hayden, C.M., Gray, D., Wanzong, S.T., Velden, C.S. and Daniels, J. 1997. Fully automated cloud drift winds in NESDIS operations. *Bull. Am. Met. Soc.*, 78, 1121-33.
- Riishojgaard, L.P. and Zhu, Y. 2004. Impact experiments on GMAO data assimilation and forecast systems with MODIS winds during MOWSAP. *Proc. Seventh Int. Winds Workshop*, 1-17 June 2004, Helsinki (EUMETSAT, ISBN, 92-9110-067-6), 281-7.
- Sarrazin, R. and Zaitseva, Y. 2004. MODIS polar winds assimilation impact study with CMC operational NWP system. *Proc. 7th International Winds Workshop*, 1-17 June 2004, Helsinki (EUMETSAT, ISBN, 92-9110-067-6), 289-96.
- Turner, J. and Warren, E. 1989. Cloud Track Winds in the Polar Regions from Sequences of AVHRR Images. *Int. J. Rem. Sens.*, 10, 695-703.
- Velden, C.S., Hayden, C.M., Nieman, S.J., Menzel, W.P., Wanzong, S. and Goerss, J.S. 1997. Upper tropospheric winds derived from geostationary satellite water vapour observations. *Bull. Am. Met. Soc.*, 78, 173-95.
- Zapotocny, T.H., Jung, J.A., Le Marshall, J.F. and Treadon, R.E. 2008. A two season impact study of four satellite data types and rawinsonde data in the NCEP Global Data Assimilation System. *Weath. forecasting*, 23, 80-100.